Time-dependent Outward Current in Guinea Pig Ventricular Myocytes

Gating Kinetics of the Delayed Rectifier

JEFFREY R. BALSER, PAUL B. BENNETT, and DAN M. RODEN

From the Departments of Medicine and Pharmacology, Vanderbilt University School of Medicine, Nashville, Tennessee 37232

ABSTRACT Several conflicting models have been used to characterize the gating behavior of the cardiac delayed rectifier. In this study, whole-cell delayed rectifier currents were measured in voltage-clamped guinea pig ventricular myocytes, and a minimal model which reproduced the observed kinetic behavior was identified. First, whole-cell potassium currents between −10 and +70 mV were recorded using external solutions designed to eliminate Na and Ca currents and two components of time-dependent outward current were found. One component was a La^{3+}-sensitive current which inactivated and resembled the transient outward current described in other cell types; single-channel observations confirmed the presence of a transient outward current in these guinea pig ventricular cells ($\gamma = 9.9$ pS, $[K]_o = 4.5$ mM). Analysis of envelopes of tail amplitudes demonstrated that this component was absent in solutions containing 30–100 μM La^{3+}. The remaining time-dependent current, I_K, activated with a sigmoidal time course that was well-characterized by three time constants. Nonlinear least-squares fits of a four-state Markovian chain model (closed − closed − closed − open) to I_K activation were therefore compared to other models previously used to characterize I_K gating: n^2 and n^4 Hodgkin-Huxley models and a Markovian chain model with only two closed states. In each case the four-state model was significantly better ($P < 0.05$). The failure of the Hodgkin-Huxley models to adequately describe the macroscopic current indicates that identical and independent gating particles should not be assumed for this K channel. The voltage-dependent terms describing the rate constants for the four-state model were then derived using a global fitting approach for I_K data obtained over a wide range of potentials (−80 to +70 mV). The fit was significantly improved by including a term representing the membrane dipole forces ($P < 0.01$). The resulting rate constants predicted long single-channel openings (>1 s) at voltages > 0 mV. In cell-attached patches, single delayed rectifier channels which had a mean chord conductance of 5.4 pS at +60 mV ($[K]_o = 4.5$ mM) were recorded for brief periods. These channels exhibited behavior predicted by the four-state model: long openings and latency distributions with delayed peaks. These results suggest that the cardiac delayed rectifier undergoes at least two major transitions between closed states before opening upon depolarization.

Address reprint requests to Dr. Dan M. Roden, Department of Pharmacology, 560 MRB, Vanderbilt University School of Medicine, Nashville, TN 37232-6602.

J. GEN. PHYSIOL. © The Rockefeller University Press · 0022-1295/90/10/0835/29 $2.00 835
Volume 96 October 1990 835–863

INTRODUCTION

For many ion channel proteins, the likelihood of conformational changes associated with gating of ion permeation is determined by transmembrane potential. A description of channel gating can facilitate characterization of the functional biological properties of these channel proteins and their interactions with ligands (Armstrong, 1975; Hille, 1977; Hondeghem and Katzung, 1977). One of the most direct ways to study ion channel gating is to record single-channel currents. However, some channels are only very infrequently recorded. For example, similar to Clapham and DeFelice (1985), we find delayed rectifier channels (I_K) in cardiac ventricular cells in only a small fraction of on-cell patches, and once identified, the channel activity disappears rapidly. In this study, we analyzed both whole-cell and single-channel currents to determine a model that describes the gating behavior of cardiac delayed rectifier channels.

Noble and Tsien (1969), using sheep Purkinje strands, demonstrated the presence of time-dependent outward current carried largely by potassium ions at voltages in the range of the action potential plateau (−40 to +20 mV). Two exponentials were required to describe the kinetics of current they measured, and the two kinetic components exhibited different rectification and ion selectivity properties. They proposed that two distinct currents, labeled I_{x1} and I_{x2}, were responsible for the time-dependent outward current. In studies of cat ventricular fibers, McDonald and Trautwein (1978) characterized the time-dependent outward current in a similar fashion. However, it has been recognized that accumulation of potassium ions in the extracellular spaces after prolonged membrane depolarization may distort the observed kinetic behavior in multicellular preparations by altering the K^+ electrochemical gradient (McDonald and Trautwein, 1978; Cohen et al., 1986). In disaggregated cells, such as canine Purkinje myocytes (Mathias et al., 1985) or guinea pig ventricular myocytes (Matsuura et al., 1987), accumulation is minimized.

Another factor complicating the kinetic analysis of delayed rectifier current in whole-cell preparations is the presence of other time-dependent currents over the "plateau" voltage range. Inward plateau currents through Ca channels or late-opening Na channels were not blocked in the early experiments and may have distorted the measurements (Cohen et al., 1986). In addition, time-dependent potassium currents, such as transient outward currents, can complicate the analysis of I_K (Clark et al., 1988); we present evidence below for a transient outward current in guinea pig myocytes. Thus, the use of single cells and block of other time-dependent currents allowed a quantitative analysis of I_K kinetics.

The parallel conductance hypothesis proposed by Noble and Tsien (1969) is not the only model that can account for the observed multiexponential behavior of this current. After addressing the accumulation problems discussed above, two groups provided evidence that the biexponential kinetics observed in activation and deactivation were not an artifact of ion accumulation (Gintant et al., 1985; Bennett et al., 1985), and further, that the observed biexponential kinetics did not necessarily result from two distinct channel types with different monoexponential kinetics activating in parallel. Bennett et al. (1985) showed that the two components of I_x shared the same reversal potential (and therefore ion selectivity), suggesting that both components

could result from the same population of channels. By separating the activating current into fast and slow exponential components, Gintant and co-workers (1985) showed that the time course of activation of the fast and slow components could not be described by the envelope of the respective fast and slow amplitude terms measured from biexponential tail currents. Hence, both groups proposed that the delayed rectifier in Purkinje cells was better described by a single population of channels having multiexponential kinetics. Further support for a model with higher-order kinetics was obtained in both guinea pig ventricle (Snyders et al., 1986; Matsuura et al., 1987) and frog atrium (Hume and Uehara, 1985; Hume et al., 1986; Simmons et al., 1986) where it was demonstrated that I_K activates with a sigmoidal time course. Two increasing monoexponential processes in parallel cannot produce such behavior.

TABLE I

State Models for Ion Channel Gating

Model	State diagram	P_{open}
1. C-O	$\text{Closed} \underset{\beta}{\overset{\alpha}{\rightleftharpoons}} \text{Open}$	$A + Be^{-t/\tau}$
2. n^2 HH	$\text{Closed}_1 \underset{\beta}{\overset{2\alpha}{\rightleftharpoons}} \text{Closed}_2 \underset{2\beta}{\overset{\alpha}{\rightleftharpoons}} \text{Open}_3$	$(A + Be^{-t/\tau})^2$
3. n^4 HH	$C_1 \underset{\beta}{\overset{4\alpha}{\rightleftharpoons}} C_2 \underset{2\beta}{\overset{3\alpha}{\rightleftharpoons}} C_3 \underset{3\beta}{\overset{2\alpha}{\rightleftharpoons}} C_4 \underset{4\beta}{\overset{\alpha}{\rightleftharpoons}} \text{Open}_5$	$(A + Be^{t/\tau})^4$
4. C-C-O	$C_1 \underset{k_{12}}{\overset{k_{21}}{\rightleftharpoons}} C_2 \underset{k_{23}}{\overset{k_{32}}{\rightleftharpoons}} \text{Open}_3$	$A + Be^{-t/\tau_1} + Ce^{-t/\tau_2}$
5. C-C-C-O	$C_1 \underset{k_{12}}{\overset{k_{21}}{\rightleftharpoons}} C_2 \underset{k_{23}}{\overset{k_{32}}{\rightleftharpoons}} C_3 \underset{k_{34}}{\overset{k_{43}}{\rightleftharpoons}} \text{Open}_4$	$A + Be^{-t/\tau_1} + Ce^{-t/\tau_2} + De^{-t/\tau_4}$

Five models for ion channel gating, and the corresponding solutions for the probability of occupying the open state (P_{open}) are shown. Each α, β, k_{ij} is a function of membrane potential. Model 1 is the simplest possible state model, models 2 and 3 are Hodgkin-Huxley (HH) models, and models 4 and 5 are general Markovian chain models.

Hodgkin and Huxley (1952) first proposed a gating model for the delayed rectifier K channel in squid giant axons. Their model provided for multiple, independent gating particles which opened and closed with first-order kinetics as functions of voltage. Gating formalisms of this type have proven useful for describing the kinetic behavior of delayed rectifier currents in many neuronal and cardiac tissue types, although the number of gating particles necessary to simulate the observed kinetic behavior has varied tremendously (from 1 to 25; see Cole and Moore, 1960; Young and Moore, 1981; Hume et al., 1986; Simmons et al., 1986; Matsuura et al., 1987; Furukawa et al., 1989). A major feature of Hodgkin-Huxley models is the constraint that the voltage-dependent rate constants must bear a fixed integral relationship to one another (α, 2α, 3α . . .; . . . 3β, 2β, β), resulting in a limited range for the system time constants.

In contrast, we (Bennett et al., 1985; Roden et al., 1988) and others (Gintant et al., 1985; Cohen et al., 1986) have considered an alternate gating scheme to account for multiexponential delayed rectifier gating in cardiac cells. Instead of postulating identical, independent gating particles within each channel, the channels were viewed as having multiple closed states in series. Similar multistate models have been used to characterize delayed rectifier gating in crayfish giant axon (Young and Moore, 1981), frog node (Palti et al., 1976), and squid axons (Conti and Neher, 1980). Like higher-order Hodgkin-Huxley models, this type of general Markovian chain allows sigmoidal activation kinetics since the channels move through multiple closed states before opening. However, no fixed relationship among the system time constants is required. Hence, models from the two classes make different testable predictions about the relationship of the system time constants at all voltages. As described further below, we found that extension of the general Markovian chain model was most consistent with our observations in guinea pig ventricular myocytes. State diagrams of models from both classes are shown in Table I.

The goal of this study was to develop a quantitative description of the gating kinetics of the delayed rectifier channel and to rule out models that were inadequate. To accomplish this, we first identified conditions under which the delayed rectifier whole-cell current could be examined in the absence of other time-dependent currents. We were then able to determine the simplest state model from the two classes described above that characterized the kinetic features observed. Once a model for channel gating was selected, we determined the voltage dependence of the rate constants and compared these kinetic predictions to delayed rectifier single channel activity recorded from on-cell patches.

METHODS

Tissue Preparation and Voltage Clamp Conditions

Ventricular myocytes were obtained from 200–300-g guinea pigs using a Langendorff perfusion technique (Farmer et al., 1983; modified as described in Roden et al., 1988). Isolated cells were stored for subsequent use at 37°C in medium 199 ($CaCl_2$ = 1.3 mM, Sigma Chemical Co., St. Louis, MO) which was supplemented with B_{12} 1 mg/liter, thyroxine 1 mg/liter, insulin 25 mg/liter, transferrin 10 mg/liter, and Na Selenite 0.01 mg/liter. Fetal calf serum 5%, penicillin 1×10^5 U/liter, streptomycin 100 mg/liter, and amphotericin B 250 mg/liter were also included. After 2–24 h of incubation, a small aliquot of cells was placed in a 0.5-ml chamber on the stage of an inverted microscope. To eliminate non-K currents during depolarizing voltage-clamp steps, cells were superfused at 1 ml/min with *N*-methyl-D-glucamine 150 mM (in some cases Tris-HCl or choline-Cl were used as NaCl replacements), KCl 4.5 mM, $MgCl_2$ 2.0 mM, $CaCl_2$ 0.1 mM, $CdCl_2$ 0.1 mM, glucose 12.5 mM, pH to 7.4 using HCl. As described further below, for experiments used to define I_K kinetics, $LaCl_3$ (0.03 mM) was added to the external solutions to remove time-dependent currents other than I_K. The bath temperature was measured with a thermistor probe, and was usually maintained at 30 ± 1°C by a Peltier-effect device (exceptions to these conditions are noted).

Delayed rectifier currents were measured using the whole-cell configuration of the patch-clamp technique (Hamill et al., 1981). It has been well established that cardiac delayed rectifier exhibits rundown with time after rupture of the membrane patch. Possible causes for this phenomenon may include allosteric effects of elevated intracellular (Mg^{2+} from the

pipette solutions (Duchatelle-Gourdon et al., 1990; bullfrog atrial cells) and wash-out of critical intermediates in the β-adrenergic pathway (Hume, 1989; guinea pig ventricular cells). Thus, for experiments aimed at accurately assessing delayed rectifier kinetics, the whole-cell voltage clamp technique was modified in a fashion similar to that described by Hume and Giles (1983) to use small electrodes, thereby minimizing rundown. Glass electrodes (borosilicate Radnoti; Glass Technology, Inc., Monrovia, CA) contained KCl 450 mM, $MgCl_2$ 2 mM, HEPES 10 mM, $CaCl_2$ 1 mM, EGTA 11 mM, MgATP 5 mM, K_2ATP 5 mM; pH adjusted to 7.2 using KOH. Tip diameters were <1 μm to minimize exchange with the cell interior and prevent net KCl accumulation; elevated KCl in the pipette provided tip resistances of 3–5 mΩ. Cells chosen for study were rod-shaped and striated, and were typically 80–120 μm in length. Conditions utilized for the cell-attached patches described below are provided in the appropriate figure legends.

Voltage Clamp

We have estimated the whole-cell voltage clamp characteristics using these electrode and cell characteristics. The response characteristics can be readily calculated given estimates of the membrane resistance and capacitance as follows (Lecar and Smith, 1985):

$$\tau = R_e C_m/(1 + R_e/C_m); \tag{1a}$$

$$V_m(\text{steady state}) = V_c R_m/(R_m + R_e). \tag{1b}$$

R_e is the access resistance, C_m is the membrane capacitance, and V_c is the clamp potential. Since the largest currents were <1 nA at the maximum clamp potential utilized (+70 mV, ~150 mV positive to E_K), the membrane resistance R_m was >150 MΩ. We assumed $C_m \leq 75$ pF (cylindrical myocyte ≤ 120 μm in length, diameter ≤ 20 μm, specific capacitance = 1 $\mu F/cm^2$) and $R_e \leq 10$ MΩ. Hence, τ was 0.71 ms (Eq. 1*a*) and steady-state V_m was +66 mV (Eq. 1*b*) when V_c was +70 mV (maximum steady-state error ≤ 4 mV).

To estimate the spatial voltage gradient along the myocyte, we calculated the space constant λ for a one-dimensional cable with diameter (d):

$$\lambda = [(d/4)(R_m^*/R_i^*)]^{1/2}. \tag{2}$$

Assuming the above maximum dimensions for a cylindrical myocyte, a specific membrane resistance (R_m^*) of 11,310 Ω-cm^2 (from R_m = 150 MΩ), and an intracellular specific longitudinal resistance (R_i^*) of 100 Ω-cm (Lecar and Smith, 1985), the space constant λ was 2,380 μm. Hence, the spatial voltage error (%) at some distance (X) from the electrode tip was $100\ (1 - e^{(-x/2380)})$. For a 120-μm cell, at the end of the cell (60 μm from the electrode), the maximum spatial voltage error was therefore ≤ 2.5%.

To directly assess the speed of the clamp, a minimally filtered (5 kHz) capacity transient was measured after a 100-mV step; a hyperpolarizing step was used to avoid possible confusion of the capacitance artifact with transient outward currents or an undescribed rapid component of I_K activation. Fig. 1 shows the current resulting from a step from −30 mV (a voltage just below the threshold for I_K activation) to −130 mV; the membrane capacitance was fully charged in <3 ms. This suggests a time constant ≤1 ms, similar to predicted value. In the whole-cell experiments described below, currents were low-pass filtered at 50 Hz (four-pole Bessel filter), and then digitized at 200 Hz. Using this filter setting, the capacity artifact was spread over 20 ms after a voltage step (Fig. 1); hence, data collected from 0 to 30 ms after a voltage clamp step were ignored. For activation steps from −70 to +60 mV, the macroscopic current 80 ms after the voltage step was <1% of steady-state; thus, the relative amount of I_K activation during the initial 30-ms period was not significant.

Normalizing Data

Whole-cell $I_K(t, V)$ data were transformed into $P_{open}(t, V)$ in the following way (Fig. 2). After 5 s of I_K activation at voltages from −20 to +70 mV, deactivating tail amplitudes were measured at −30 mV (tail amplitude = difference between current measured at $t = 25$ and $t = 5{,}000$ ms at −30 mV). Since these tail amplitudes reflect steady-state I_K activation at the preceding voltage, the appropriate scaling factors between current and voltage were derived using nonlinear regression (SIMPLEX; Nelder and Mead, 1965) to fit the following Boltzmann equation to the tail amplitudes:

$$I_K(t, V) = I_{Kmax}/[1 + \exp((V_h - V)/sf)]. \quad (3)$$

In this equation, V_h is the half-maximal voltage, I_{Kmax} is the fitted maximal current corresponding to 100% of the channels open, and sf is a slope factor. These three parameters (I_{Kmax}, V_h, and sf) were then used to scale all whole-cell currents from a given experiment into open channel probabilities. We assume $P_{open} = 1.0$ when $I = I_{Kmax}$; hence, $P_{open}(t, V) = I_K(t, V)/I_{Kmax}$. Eq. 3 is the solution for the steady-state partitioning of a system between two states. Although we consider models with more than two states in our kinetic analysis, the system can apparently be partitioned at steady-state into two pools, open and not open (Fig. 2); thus, Eq. 3 was used to normalize the data.

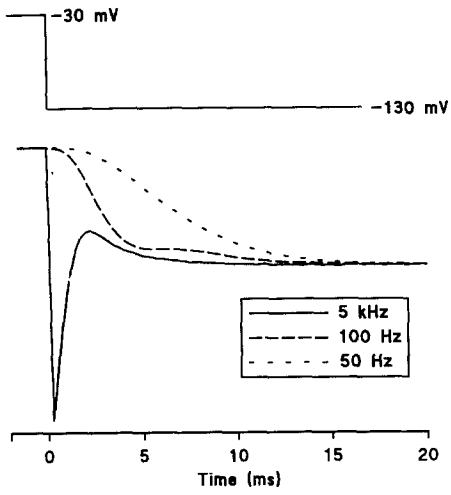

FIGURE 1. Response of the voltage clamp circuit to a −100 mV step command (electrode resistance 5 MΩ, cell length ~ 120 μm). The relatively unfiltered response (four-pole Bessel filter, cutoff frequency 5 kHz) is shown, along with two filtered responses (50, 100 Hz). In the unfiltered response, the downward time-dependent current following the rapid inward capacity transient represents I_{K1} activation at −130 mV. At higher filter settings (50–100 Hz), the current measurement is distorted for 15–20 ms.

Fitting Analytical Solutions for Gating Models to P_{open} Data

For all of the gating models examined, the solution for the time course of occupying the open state at any one voltage may be expressed as a specific combination of time constants and amplitude terms. We used the SIMPLEX regression technique to fit the solutions given in Table I for n^2 and n^4 Hodgkin-Huxley models and three- and four-state Markovian chains to the macroscopic time course of the activating delayed rectifier currents. Since the n^2 Hodgkin-Huxley and three-state Markovian chain models were subsets of the four-state general Markovian chain (model 5, Table I), they were "nested" and therefore could be compared to the more general model using a test for nested model discrimination (Horn, 1987). If n data points are fitted with two models A and B, and if model A has residual sum-of-squares error

SSE_A and a free parameters and is a restricted subset of model B (with sum-of-squares error SSE_B and b free parameters), then the statistic T comparing the two models is defined as follows:

$$T_{a,n-b} = [(SSE_A - SSE_B)/SSE_B] \cdot [(n - b)/a)]. \quad (4)$$

The T statistic has an F distribution and may therefore be compared to tabulated values at specific α levels of significance. At each voltage, fits of the reduced models (models 2 and 4 in Table I) were compared to that for the full model (model 5 in Table I). Since more than two models were fit to each data set, the full model was deemed to provide a significantly better fit at a particular voltage at the 0.05 level only if the T statistic was associated with a P

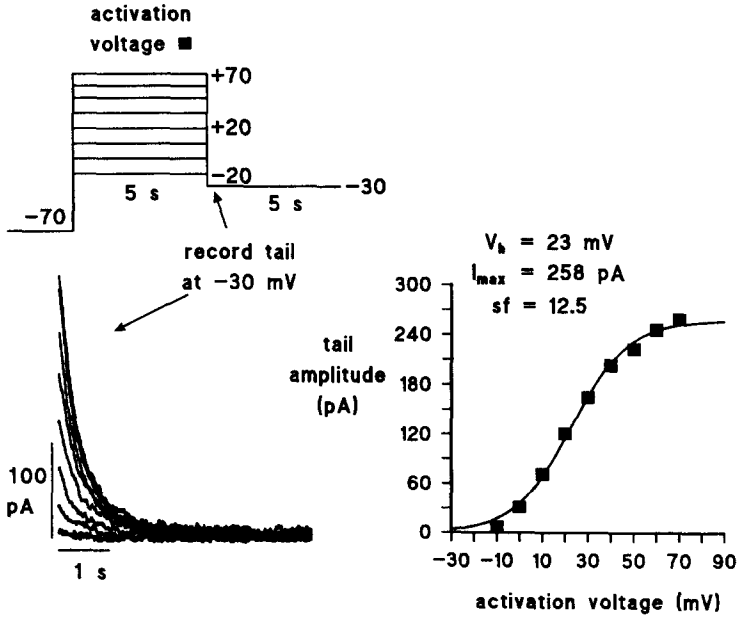

FIGURE 2. (*Left*) After 5 s of I_K activation at voltages from −20 to +70 mV, deactivating tail amplitudes were measured at −30 mV. The voltage clamp protocol is shown (*top*) with the resulting tails elicited at −30 mV below. Tail amplitudes (tail amplitude = difference between I measured at $t = 25$ and at $t = 5000$ ms at −30 mV) increased as the preceding activating voltage increased, with saturation at +70 mV in this experiment. (*Right*) The tail amplitudes were then fitted to a Boltzmann distribution (Eq. 3).

value < 0.01 for all six data sets at that voltage (Godfrey, 1985). Since the error distributions were unknown, the unweighted sum-of-squares error was used as a fitting criterion. To the extent that the error standard deviations are not constant, the validity of the sum-of-squares as a maximum likelihood estimator decreases. However, this does not compromise our conclusions because in all cases the best model was obvious from visual inspection.

Rate Constant Estimation through Global Fitting

All of the Hodgkin-Huxley models shown above have solutions for the probability of channel opening that are functions of only two independent rate constants (α and β, see state models

1, 2, and 3 in Table I). However, large numbers of independent rate constants are present in the general Markovian chain models (k_{ij}, see models 4 and 5, Table I); for such models with more than two states, the voltage-dependent rate constants are underdetermined at any single voltage. For example, model 5 contains four independent states, and is therefore described by a system of four first-order differential equations (functions of voltage) with six unknown rate constants. Hence, unlike the Hodgkin-Huxley models, unique values for the rate constants cannot be determined by fitting data at only one voltage (four equations, six unknowns). To overcome this obstacle, we utilized a numerical approach which allows global determination of the rate constants from macroscopic currents over a wide range of voltages (Balser et al., 1990).

To determine the values of the rate constants over a range of voltages, the rate constants were parameterized as exponential functions of voltage as follows:

$$k_{ij} = \exp(A_{ij} + B_{ij}V + C_{ij}V^2). \tag{5a}$$

This is a form of the equation given by Stevens (1978). The A term reflects the generalized attempt frequency for transiting the energy barriers that separate the channel conformations as well as the free energy barriers that exist in the absence of an electric field. The B term reflects the effect of the membrane field on the free energy difference between a given conformation i and the transition from state j, and C reflects the field-induced dipole effects which allow rate constants to saturate and/or reverse direction as a function of voltage. We have examined a simpler parameterization for the rate constants as well:

$$k_{ij} = \exp(A_{ij} + B_{ij}V). \tag{5b}$$

This parameterization, which omits the influence of field induced dipole effects, is a subset of Eq. 5*a;* sum of square errors derived from fitting data sets to both parameterizations can therefore be compared using the T statistic (Eq. 4) as described above for distinguishing among nested models.

The global fitting procedure determines the parameters A_{ij}, B_{ij} . . . which define the model rate constants over a range of potentials. For the four-state model, using the parameterizations given by Eq. 5*a* for each of the 6 rate constants would provide a total of 18 unknown parameters (six unknown rate constants k_{ij}, each determined by the three parameters A_{ij}, B_{ij}, C_{ij}). By fitting this model to data collected over at least five voltages, 20 equations would be generated, and the unknown parameters would no longer be underdetermined. For the global fits described below, data collected at a minimum of 14 voltages were used.

Details of the global fitting procedure have been reported previously (Balser et al., 1990). In brief, a numerical integrator was used to calculate the open state occupancy for a given set of rate constants (LSODA; Hindmarsh, 1983; Petzold, 1983). To compare the calculated open state occupancy to the data and update the parameters, a modified SIMPLEX algorithm (Nelder and Mead, 1965) for minimizing the residual sum of squares was used. Each time the parameter search converged, the procedure automatically restarted using the parameters of best fit as initial guesses until the same minimum SSE for the fit was obtained to within 0.00001 on two consecutive searches, thereby maximizing the likelihood of convergence at the global minimum. In general, up to 20,000 iterations were necessary before the parameters of best fit were obtained. Because of the long execution times intrinsic to the global fitting procedure (3–6 d of computation per data set using a COMPAQ (Houston, TX) 386 20-MHz PC with model 80387 coprocessor support and NDP 32-bit FORTRAN, Phar Lap Software, Inc., Cambridge, MA), data sets were reduced such that the macroscopic current at each voltage contained 30 points, with points divided equally among first approximations to the three time constants (200, 1,000, and 5,000 ms). Global fits for determination of rate constants were

performed using complete data sets from six different cells. Grouped data are reported as mean ± 1 SE unless otherwise specified.

Analysis of Single-Channel Data

Data were analyzed with custom software written in BASIC (Microsoft, QuickBASIC) which allowed digital filtering, generation of amplitude histograms, and event detection based on a half-amplitude criterion (Colquhoun and Sigworth, 1983). Amplitude histograms were fitted to sums of gaussians using the SIMPLEX algorithm for minimizing the sum-of-squares. For multichannel patches, open times were determined by using a first-open, first-closed scheme. We have found this method provides similar results to other methods using random assignment of closures to openings. Exponential functions were then fitted to open times using the SIMPLEX algorithm. Probability of opening versus time ensembles were calculated by dividing the ensemble average current from a series of recorded current sweeps by the estimated single channel current and the number of channels in the patch. The number of channels in a patch was estimated by using binomial analysis as described in detail by Patlak and Horn (1982). For analysis of the time to first opening, we used the half-amplitude criterion (two consecutive samples greater than or equal to one-half the unitary current amplitude) and ignored sweeps that contained no openings. The resulting latency histograms were scaled into probability density by dividing by the total number of latencies and the bin size. Using the rate constants determined previously from the global fits to the six sets of whole-cell data, we predicted the times to first opening by assuming the open state of model 5 (Table I) was an absorbing state ($k_{34} = 0$), as described by Patlak and Horn (1982). Numerical integration was then used to calculate the cumulative distribution functions for the probability that channels were open as of time = t; the distributions calculated from each of the six sets of fitted rate constants were then averaged, and the mean distribution was corrected for channel number (Patlak and Horn, 1982; Eq. A17) and the temperature difference between the whole-cell and single channel records ($T = 22$°C for single channels, $T = 30$°C for whole-cell currents; $Q_{10} = 3$). Using a Lagrange interpolation algorithm (Shoup, 1983), the average cumulative distribution was then converted to a probability density function for comparison to the experimentally measured times to first opening.

RESULTS

Examination of Time-dependent Outward Current Components

Although our external solutions were extensively modified by Na^+ removal, lowered Ca^{2+}, and addition of Cd^{2+} to eliminate inward currents, we could not exclude the possibility of outward, time-dependent currents other than I_K. We therefore performed "envelope tests" (Noble and Tsien, 1969); current tail amplitudes at −30 mV after depolarizing pulses of increasing duration were compared to the current measured directly during the longest depolarizing pulse. Fig. 3 shows an envelope test performed at +50 mV. The current tail amplitudes increased more rapidly than the developing current during the step to +50 mV; the same discrepancy was consistently noted at +20 mV. Hence, the two measurements of activation exhibited kinetic differences, suggesting the presence of multiple time-dependent outward currents. When La^{3+} was superfused, there was a reduction in the current tail amplitudes (●, Fig. 3); the effect on tail currents following brief depolarizations (<2 s) was greater than on those after longer depolarizations (>2 s). In the absence of La^{3+}, the envelope test at +50 mV was never satisfied (six of six experiments),

whereas in the presence of La^{3+} the envelope test was satisfied (30–100 μM, four of four experiments; 10 μM, two of four experiments), suggesting that in the presence of La^{3+}, the time-dependent outward current is produced by a single class of K channels.

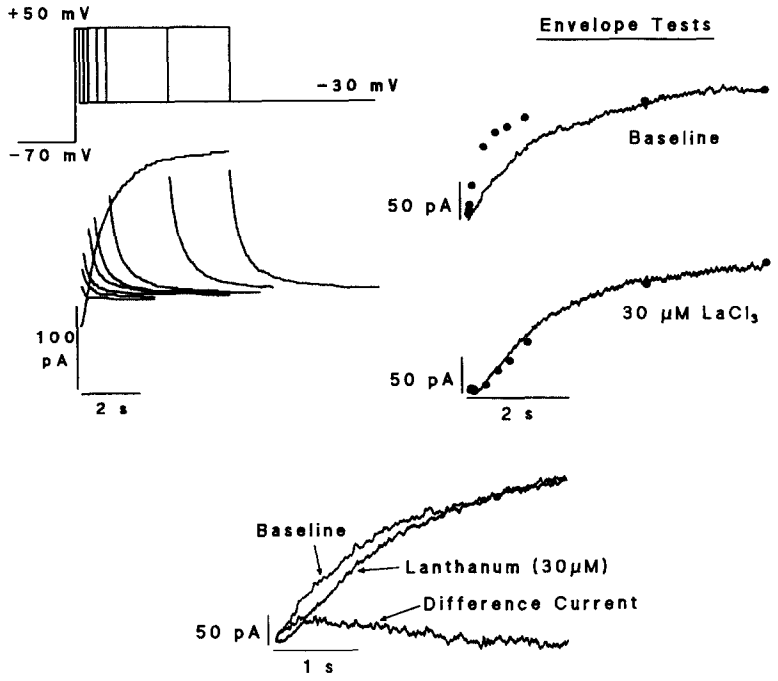

FIGURE 3. An envelope test performed at +50 mV. (*Top, left*) Steps of increasing duration to +50 mV were followed by 5-s steps to −30 mV; the currents elicited by the 5-s step to +50 and all steps to −30 mV are shown. The electrode contained KCl 150 mM, $MgCl_2$ 2 mM, $CaCl_2$ 1 mM, HEPES 10 mM, EGTA 11 mM, MgATP 5 mM, K_2ATP 5 mM; pH adjusted to 7.2. The external $[K^+]$ was 4.0; bath temperature was 30°C. (*Top, right*) Similar envelope tests were performed in the absence and presence of 30 μM $LaCl_3$ (here $T = 25$°C). Time-independent currents have been subtracted, and the activating current at +50 mV in La^{3+} was scaled by 1.61 to correct for rundown during the control (pre-La^{3+}) period. (●) Tail current amplitudes that have been scaled by a factor such that the two measurements coincide at the 6-s time point (scaling factors: baseline tails × 1.14; La^{3+} tails × 2.86). (*Bottom, middle*) The same activating currents at +50 mV measured before and during La^{3+} superfusion are shown superimposed. The La^{3+}-sensitive current (baseline minus corrected current in La^{3+}) is also shown.

At the bottom of Fig. 3 the activation of time-dependent outward current measured directly at +50 mV is shown before and after the addition of La^{3+}, along with the La^{3+}-sensitive current. At concentrations from 10–30 μM, La^{3+} had little or no effect on the magnitude of the steady-state outward current at positive voltages,

suggesting that La^{3+} does not reduce I_K. The time course of the La^{3+}-sensitive current shown in Fig. 3 resembles that of a transient outward current. In fact, in experiments aimed at characterizing single potassium channels in guinea pig ventricular cells using cell-attached patches with physiological external K^+ concentrations, a potassium channel has been identified which inactivates in the manner expected for a transient outward current (Fig. 4). By using voltage ramps during episodes of channel opening, we have measured a slope conductance of 9.9 pS and a negative reversal potential (−50 mV, $[K_o] = 4.5$ mM), suggesting that the channel predominantly conducts potassium ions. We have not been able to determine whether this K channel is La^{3+}-sensitive; its frequency of appearance in on-cell patches is low, consistent with reports that transient outward current is not usually observed in these cells (Josephson et al., 1984).

Evaluation of I_K Gating Kinetics

Fig. 5 shows I_K (30 μM La^{3+} present) recorded from a voltage-clamped guinea pig ventricular myocyte. After 4 s at −70 mV, the cell was clamped to one of the activating voltages indicated. Two features of I_K activation are apparent. First, I_K activation is sigmoidal, as previously noted in guinea pig ventricular cells (Snyders et al., 1986; Matsuura et al., 1987). Secondly, I_K activation contained a relatively slow component; the current was still increasing after 5 s of activation. We tested whether two Hodgkin-Huxley models (Table I) could simulate the observed kinetic behavior; the n^2 (model 2) and n^4 (model 3) Hodgkin-Huxley models were examined. Although both models provided good simulations of I_K activation at −10 to +20 mV, at higher voltages they did not describe the data well. Increasing the power of the activation variable from 2 to 4 did not appear to improve the fits. When the data set was reduced to include only the early part of I_K activation (the first 1,000 ms), an n^2 model provided a good approximation to the data at all voltages tested (Fig. 5, *bottom right*).

Next, the three-state Markovian chain model (Table I, model 4) was tested. This model approximated the data well (Fig. 6 *a*); examination of the fitted parameters revealed two activation time constants which differed by nearly an order of magnitude (τ_1, τ_2 = 301 ± 129, 1840 ± 415 ms at +40 mV; n = 6). However, expanding the first 500 ms of the fit indicated that the sigmoidal nature of I_K activation was not well simulated by this model (Fig. 6 *a, top right*). When only the first 1,000 ms of the same data set were fitted (Fig. 6 *a, bottom right*), the early period of activation was well simulated (τ_1, τ_2 = 80 ± 10, 569 ± 35 ms at +40 mV; n = 6). This analysis suggests that a model which simulates all the essential kinetic features of I_K activation must have at least three time constants which may vary over a range of two orders of magnitude. The simplest model which met these requirements was the four-state Markovian chain (Table I, model 5). This model reproduced all of the features of the data, including the sigmoidal nature of I_K activation, at all voltages tested (Fig. 6 *b*). As suggested above, the three system time constants varied by up to two orders of magnitude (τ_1, τ_2, τ_3 = 61 ± 13, 555 ± 49, 5,231 ± 1,554 ms at +40 mV; n = 6).

The sum-of-square errors from fits of the four-state Markovian chain model were

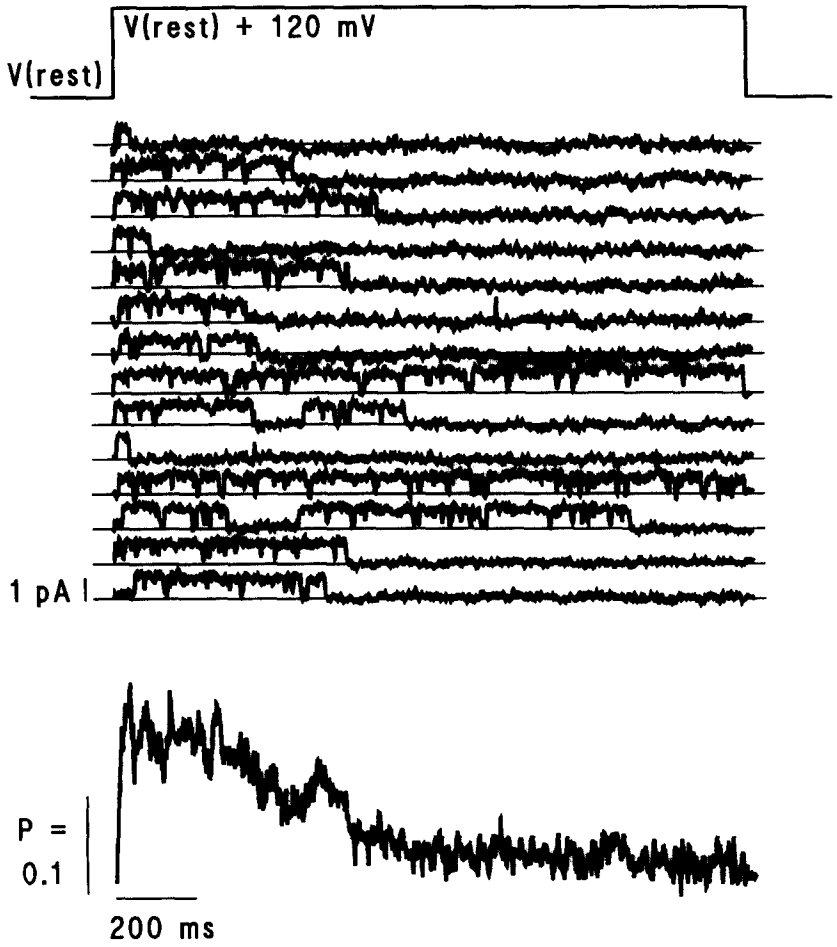

FIGURE 4. (*Top*) A cell-attached patch clamped to a potential 120 mV positive to V_{rest} (V_{rest} approximately −80 mV from whole-cell experiments) and displaying outward unitary current (filtered at 200 Hz, sampled at 1 KHz). The bath contained NaCl 145 mM, KCl 4.0 mM, $MgCl_2$ 1.0 mM, $CaCl_2$ 1.8 mM, HEPES 10 mM, glucose 10 mM; pH 7.40; T = 27.5 ± 1°C. The 5-MΩ patch electrode contained *N*-methyl-D-glucamine 150 mM, $MgCl_2$ 5 mM, $CaCl_2$ 0.1 mM, $CdCl_2$ 0.1 mM, $LaCl_3$ 0.1 mM, KCl 4.5 mM, HEPES 10 mM, glucose 12.5 mM; pH 7.40 with HCl. 14 of 64 consecutive sweeps are shown; the remaining 50 sweeps contained no openings. (*Bottom*) Ensemble average of the 64 sweeps, scaled into open channel probability by assuming only one channel in the patch and a unitary current of 0.85 pA.

compared to those from the simpler models using a $P < 0.01$ criterion for significance (see Methods). The four-state model was significantly better than the n^2 Hodgkin-Huxley model at +10 to +70 mV in six of six data sets; it did not, however, show a statistical improvement over the n^2 model in one of six data sets at 0 and −10 mV. Although the n^2 and n^4 Hodgkin-Huxley models both have two degrees of freedom (α, β), the n^4 model cannot be compared to the four-state Markovian chain using the T statistic for nested model comparison (Eq. 4) since it has five states (Table I)

and is therefore not a subset of the four-state model; however, at all voltages, in six of six data sets, the sum-of-squares errors for the n^4 model were greater than or equal to those for the n^2 model. The four-state model provided a significantly better fit than the three-state Markovian chain at +30 to +70 mV in six of six data sets; however, it did not show improvement over the three-state model in one of six data sets at +20 mV, three of six data sets at +10 mV, four of six data sets at 0 mV, and five of six data sets at −10 mV. Thus, the four-state model was superior to both the Hodgkin-Huxley n^2 and n^4 models and the three-state Markovian chain model.

Rate Constant Estimation through Global Fitting: Predictions of Single Channel Behavior

In order to derive rate constants for the four-state Markovian chain, the model was fitted to each of six sets of macroscopic current data obtained from six different

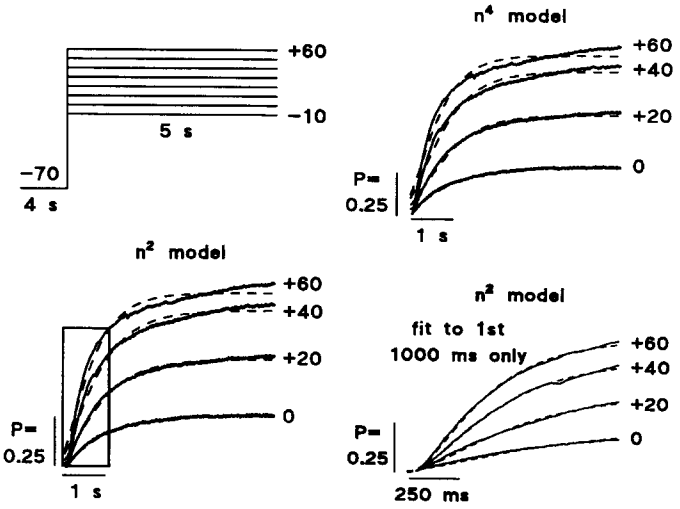

FIGURE 5. Fits of n^2 (*bottom, left*) and n^4 (*top, right*) Hodgkin-Huxley models to I_K activation at 0, +20, +40, and +60 mV (similar data were obtained at −10, +10, +30, +50, and +70 mV).(*Top, left*) The voltage clamp protocol is illustrated. Macroscopic currents were scaled into open channel probabilities using the approach described (Fig. 2). Data are shown by the solid lines, while least-squares fits are shown by the dashed lines. (*Bottom, right*) Fits to only the first 1,000 ms of I_K activation (box in bottom left panel) using a Hodgkin-Huxley n^2 model.

guinea pig ventricular myocytes. Three voltage clamp protocols were used to obtain data from −80 to +70 mV. These voltage clamp protocols, one of the six data sets obtained (*open circles*), and the least squares global fit to that data set (*solid lines*) are shown in Fig. 7. One protocol (*top left*) was used to obtain kinetic information during I_K activation (clamp at −70 mV, step to +10 to +70 mV), whereas another protocol (*top right*) was used to obtain similar information during I_K deactivation (clamp at −70 mV, step to +50 mV for 5 s, then step to +10 to −50 mV). Since I_K is small at voltages near E_K, the latter protocol was inadequate for obtaining kinetic information below −50 mV. Therefore, a paired pulse protocol (Fig. 7, *bottom*) was used. I_K

was activated for 10 s at +50 mV, and then deactivated for various test intervals at −80 mV. After the test interval, I_K was activated at +20 mV for 400 ms and the resulting current collected for the global fitting procedure. Using this procedure, currents at +20 mV were larger after short times at −80 mV than after long times, reflecting the time course of deactivation of I_K at −80 mV. Kinetic information was obtained at −60 mV in four of six experiments in a similar fashion. The global fit shown in Fig. 7 resulted from using the three-parameter expression for the rate constants (Eq. 5*a*). The two-parameter expression which omits the dipole term $C_{ij}V^2$ (Eq. 5*b*) was also fitted to each of the six data sets. Table II shows the sum of squares errors obtained from fitting each of the data sets using both parameterizations.

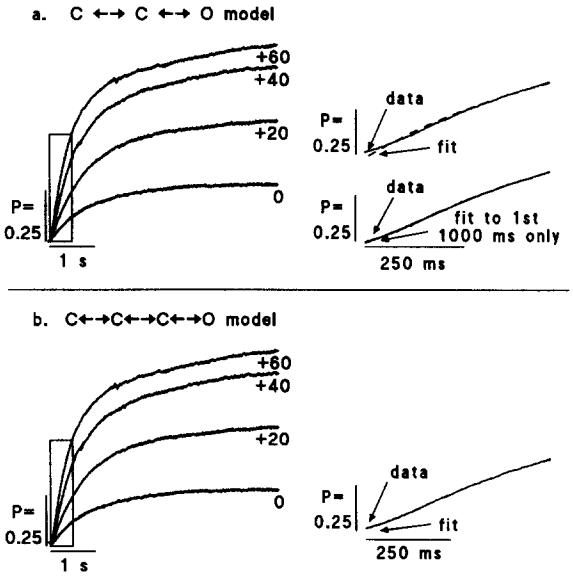

FIGURE 6. (*a*) Fits of a three-state C-C-O model to I_K activation. (*Left*) Fits to 5,000 ms of activation at four voltages. At +40 mV τ_1, τ_2 = 483, 3,053 ms. (*Top, right*) The first 500 ms of the fit to 5,000 ms of data at +40 mV is expanded to show the inadequacy of the model at the onset of activation. (*Bottom, right*) The first 1,000 ms of data at +40 mV was refitted to the same model; τ_1, τ_2 = 74, 446 ms. (*b*) Fits of a four-state C-C-C-O model to I_K activation. (*Left*) Fits to 5,000 ms of activation at four voltages. At +40 mV τ_1, τ_2, τ_3 = 54, 413, 2,357 ms (*right*) The first 500 ms of the fit to 5,000 ms of data at +40 mV is expanded to show the adequacy of this model for simulating the earliest phase of activation.

These were compared using the T statistic (Eq. 4) as described above for distinguishing among nested models. In six of six experiments, the three-parameter expression was significantly better ($P < 0.01$).

The globally fitted rate constants for all six data sets using the three-parameter expression are summarized in Fig. 8. These rate constants were used to predict the steady-state P_{open} (t = 200 s) vs. voltage relationship and the mean open times for single channels (Fig. 9). The half-maximal voltage was 26 mV, and the slope factor was 13.5. The predicted open time at 0 mV was 1 s and increased as the voltage became more positive. The uncertainty in the open time at positive voltages depended on the uncertainty in rate constant k_{34} at these voltages (Fig. 8).

Single-Channel Delayed Rectifier Recordings

On two occasions (from 263 attempts) we have succeeded in recording single channels for brief (4–5 min) periods in cell-attached patches (Fig. 10, conditions given in figure legend) which exhibit the kinetic behavior expected for a delayed rectifier channel. To activate channels, patches were stepped from the cell resting potential to a potential 140 mV positive, causing outward unitary currents which

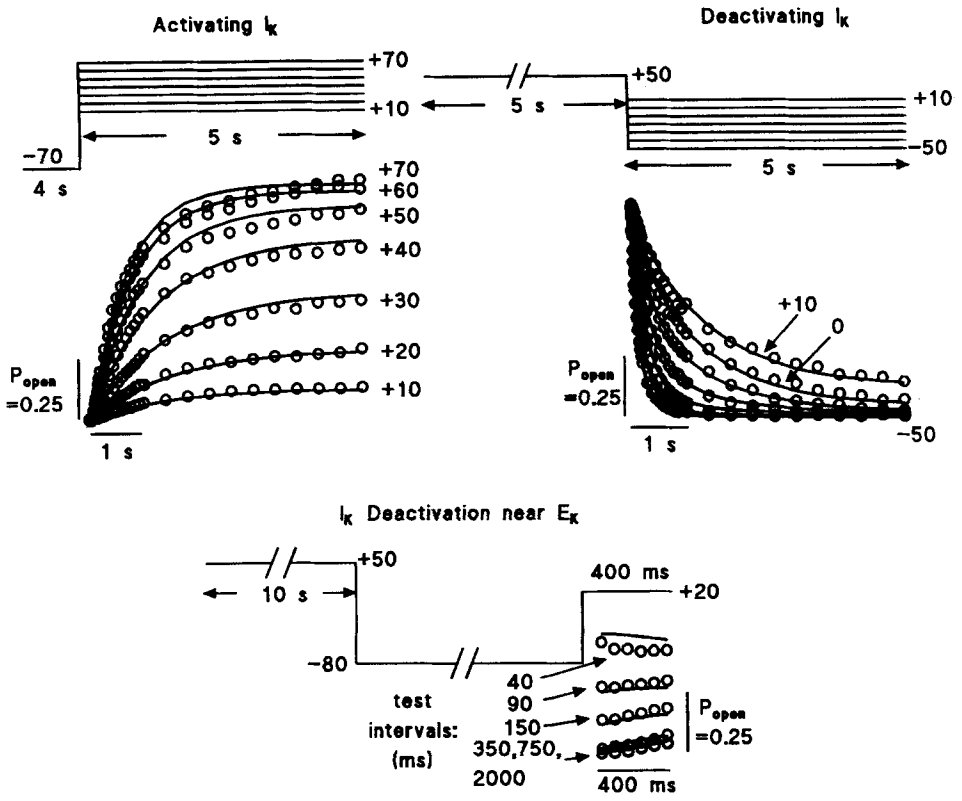

FIGURE 7. Three types of voltage clamp protocols used to generate data sets for global fits to I_K (described in text). The open circles show a reduced data set obtained from a voltage-clamped guinea pig myocyte, and the lines indicate the least-squares global fit to these data using the four-state general Markov model (C-C-C-O). To ensure representation of all kinetic components, the reduced data set (see Methods) contains 30 data points, with 10 points each in the first 200, 1,000, and 5,000 ms.

activated after a delay. Since physiologic external and pipette potassium concentrations were used ($[K]_o$ = 4.5 mM), there is uncertainty in the clamp voltage since the resting potential is unknown. However, in the whole-cell experiments reported here, using similar external solutions, the zero-current potential was −81 ± 3 mV (n = 6). Hence, we estimate that the unitary currents were recorded at a membrane potential of approximately +60 mV. Binomial analysis (Patlak and Horn, 1982) indicated that

one patch (left) had three channels and the other (right) had two channels. Subconductance levels were also seen (e.g., Fig. 10 *left*, sixth sweep from the top). Ensemble probabilities for channel opening are given below the respective single-channel sweeps, and are corrected for channel number and unitary current estimated from amplitude histograms (see below). These ensembles were calculated from 29 sweeps recorded from the three-channel patch and 21 sweeps from the two-channel patch.

Amplitude histograms for both patches at ~+60 mV are shown in Fig. 11 (*top*). The open amplitudes were estimated from fitting the histograms to sums of gaussians (see Methods). For the three-channel patch (*left*), the predominant open amplitude was ($\mu \pm$ SD) 0.81 ± 0.13 pA (estimated chord conductance = 5.7 pS), with double openings occurring at 1.5 ± 0.29 pA. The two-channel patch (*right*) contained a predominant open amplitude of 0.70 ± 0.11 pA (estimated chord conductance = 5.0 pS). Histograms showing the time to first opening for both

TABLE II

Comparison of Global Fits Using Two- and Three-Parameter Expressions for the Rate Constants

Cell no.	SSE		No. of data pts.	T
	Three-parameter	Two-parameter		
1	0.472	0.600	506	10.82
2	0.552	1.118	506	41.01
3	0.332	0.457	506	15.06
4	0.367	0.515	506	16.24
5	0.218	0.296	470	13.32
6	0.274	0.324	470	6.717
				$T_{0.01} = 2.32$

Minimum sum-of-squares errors (SSE) for six experiments where two- and three-parameter expressions defining the voltage dependence of the rate constants were utilized. The three-parameter fits were statistically better than the two-parameter fits at $P < 0.01$ in six of six cells. T statistics were calculated using Eq. 4.

patches are shown in Fig. 11 (*bottom*) after scaling into probability density (bin width 90 ms). The three-channel patch provided 20 latencies, and the two-channel patch provided 14. The superimposed solid lines indicate the predicted latency distribution from global fits to the whole-cell delayed rectifier currents using the C-C-C-O model.

Visual inspection of the records shown in Fig. 10 indicates multiple types of opening behavior for these channels. There are long openings (≥500 ms) which are separated by gaps in channel activity, as well as brief open events (tens of milliseconds) which occur both in isolation and between intermittent brief closures within some of the long openings. Both patches contained both types of openings; therefore, in order to generate enough events to evaluate these components, the open times from both patches were pooled. Fig. 12 (*left*) shows the distribution of open times. These were fitted to a two exponential function (■, Fig. 12, *right*); the fitted time constants were $\tau_1 = 70$ ms, $\tau_2 = 642$ ms. The first component is

illustrated by the solid line (Fig. 12, *right*); the second exponential was underestimated due to the low number of events and the length of the clamp step which interrupted some of the openings (2 or 3.5 s; see Fig. 10) and is therefore not graphed.

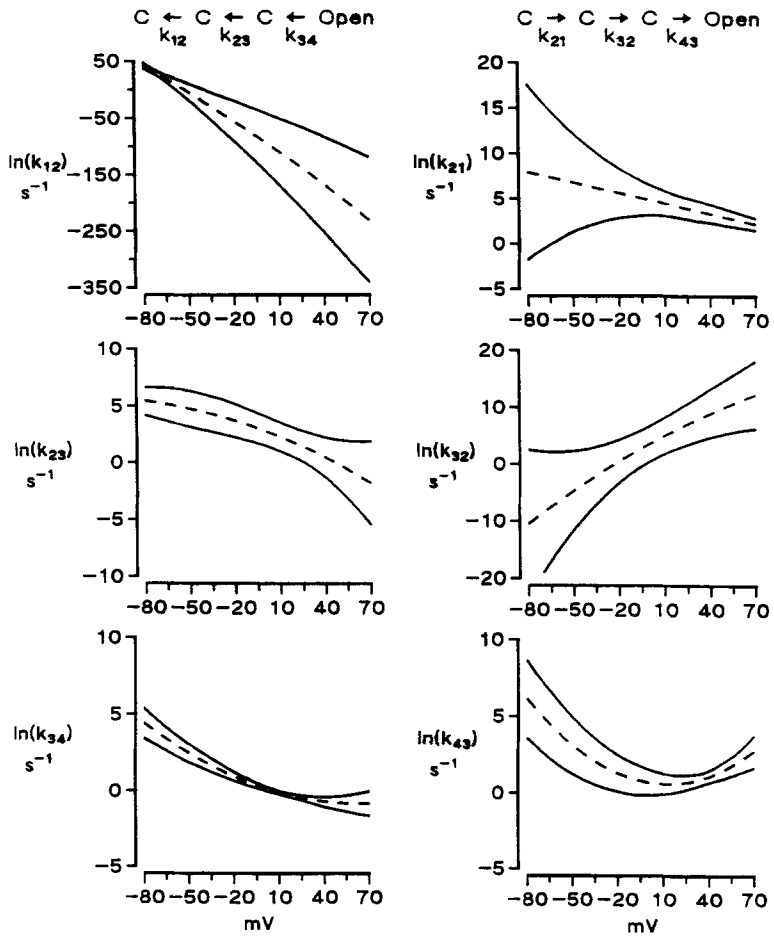

FIGURE 8. Mean values (*dashed lines*) and standard errors (*solid lines*) of rate constants obtained from global fits to six sets of experimental data using C-C-C-O model. (*Left*) Rate constants controlling movement away from the open state. (*Right*) Rate constants controlling movement toward the open state.

DISCUSSION

In these studies we have established conditions whereby the delayed rectifier can be studied in the absence of other time-dependent currents, proposed a minimal model which accounts for the kinetic features that we have observed, and have compared

this model to other proposed gating models for this channel. We have used a procedure for global parameter estimation to determine the voltage dependence of the rate constants for the model we have proposed. Finally, we have used these rate constants to make predictions regarding single-channel behavior, and have compared the predictions with recordings from delayed rectifier single channels in cell-attached patches.

Resolution of Multiple Components of Time-dependent Outward Current

The envelope test indicated that multiple components of time-dependent outward current were present in these cells (Fig. 3). Steps above E_K are known to elicit decaying outward currents through inwardly rectifying K channels (Matsuda and Noma, 1984; Saigusa and Matsudal, 1988); however, this current inactivates rapidly ($\tau < 5$ ms). Other potassium channels that exist in mammalian heart, such as transient outward or Ca^{2+}-activated currents, may make contributions to the time-dependent outward current in guinea pig ventricle. Lanthanum removed the extra component(s) of time-dependent outward current; further, the lanthanum-

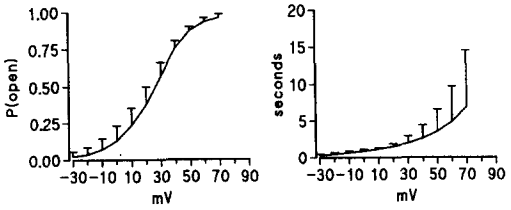

FIGURE 9. (*Left*) Steady-state P_{open} vs. voltage predicted from six sets of fitted rate constants (C-C-C-O model). Steady-state open probability for each set of fitted rate constants was calculated by numerically solving for the probability of channel opening at $t = 200$ s. (*Right*) Predicted mean channel open time as a function of voltage. These values were obtained by taking the average of the inverse of the rate constant leaving the open state for the six whole-cell experiments.

sensitive current during a step to +20 mV rapidly activated and then inactivated, suggesting block primarily of a transient outward current. Aside from this pharmacological evidence, we have presented single-channel data (Fig. 4) which directly confirm the presence of an inactivating channel that would produce a transient outward component of macroscopic current. For reasons that are unclear, the magnitude of this current is variable; this variability may explain the absence of this current in guinea pig ventricular myocytes in earlier reports (Josephson et al., 1984). Other investigators have recently also described multiple components of time-dependent outward K current in this cell type (Sanguinetti and Jurkiewicz, 1990).

It is possible that activation of the La^{3+}-sensitive current is Ca^{2+}-dependent, since lanthanum is known to deplete sarcoplasmic reticulum calcium stores (Wendt-Gallitelli and Isenberg, 1985) and to displace Ca^{2+} from cell surface sites (Kim et al., 1987). Transient outward currents are known to have Ca^{2+}-sensitive and Ca^{2+}-insensitive components (Coraboeuf and Carmeliet, 1982). However, we cannot rule out direct blockade of this transient outward conductance by the trivalent cation. The effect of La^{3+} on delayed rectifier currents appeared to be minimal; at +50 mV, La^{3+} had little or no effect on the total time-dependent current developing during

long depolarizations, which primarily reflects I_K. The delay present in the activation of time-dependent outward current when La^{3+} is present (Fig. 3) thus reflects suppression of transient outward current(s) which contaminate measurement of I_K after brief times at positive voltages, and not a direct effect of La^{3+} on the delayed rectifier.

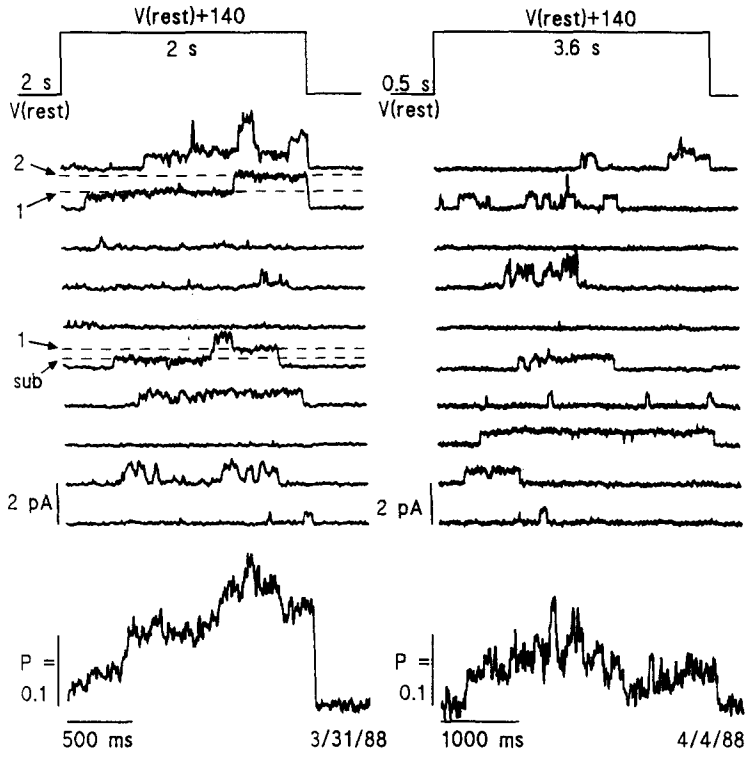

FIGURE 10. (*Top*) Unitary currents recorded from two different cell-attached patches (*left* and *right*). Patch electrodes and the bath both contained *N*-methyl-D-glucamine 150 mM, $MgCl_2$ 2 mM, $CaCl_2$ 0.1 mM, $LaCl_3$ 0.1 mM, $CdCl_2$ 0.1 mM, KCl 4.5 mM, HEPES 10 mM, glucose 12 mM, (±) isoproterenol 0.002 mM; pH 7.35; $T = 25 \pm 1$°C. To activate channels, patches were stepped from their resting potential (~ −80 mV) to a potential 140 mV positive, causing outward unitary currents which activated with a delay. Binomial analysis indicated that one patch (*left*) had three channels and the other (*right*) had two channels. A possible substate opening is noted in the figure. (*Bottom*) Ensemble averages (P_{open}) for the two patches, corrected for channel number and the unitary currents calculated from amplitude histograms (see Fig. 11). These ensembles were calculated from 21 sweeps recorded from the two-channel patch, and 29 sweeps from the three-channel patch.

Evaluation of I_K Gating Kinetics

In calf Purkinje strands (Bennett et al., 1985) and single Purkinje myocytes (Gintant et al., 1985), two time constants were resolved in the macroscopic deactivation of delayed rectifier currents; additionally, Gintant et al. (1985) were able to resolve two

time constants during activation. In neither case was a fixed integral relationship between the time constants observed. Since the simplest state model (closed – open; Table I) predicts only one time constant, and since the simplest state model with two time constants has three states, both groups expressed the gating reaction with two closed states before opening in the form of a general multistate Markovian chain (model 4, Table I). Although Gintant et al. (1985) detected two components of

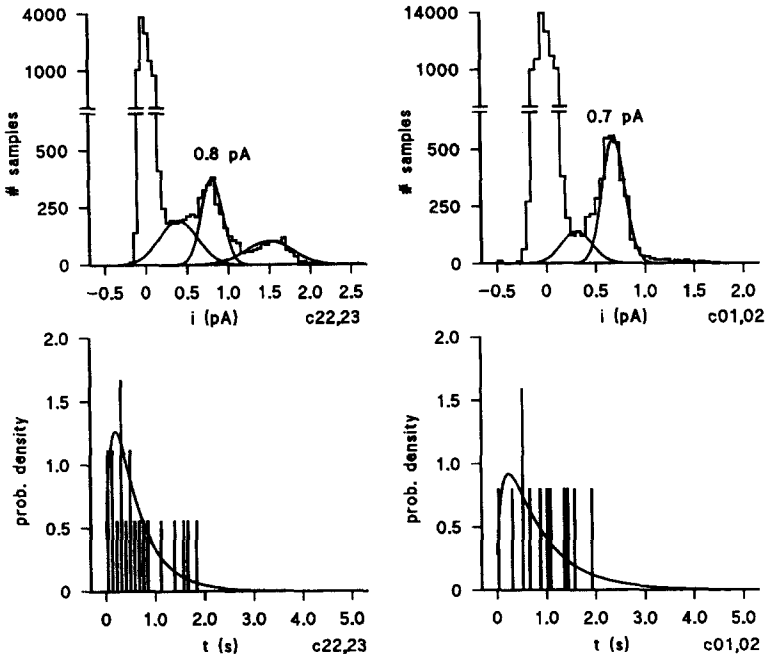

FIGURE 11. (*Top*) Amplitude histograms for the three-channel patch (*left*) and two-channel patch (*right*) from Fig. 10. The predominant unitary current levels were 0.8 and 0.7 pA, respectively, as assessed by least-squares fits to Gaussian curves (shown superimposed); the clamp potential was V_{rest} + 140 mV (~+60 mV) in both experiments. Gaussian curves for lower amplitude openings were included; these intermediate peaks suggest openings to sublevels. (*Bottom*) Histograms showing time to first opening for both patches are shown after scaling into probability density (bin width 90 ms). The three-channel patch provided 20 latencies, and the two-channel patch provided 14 (null sweeps were ignored). The solid lines indicate the predicted latency distribution from the global fits to the whole-cell delayed rectifier currents using the C-C-C-O model. These curves have been corrected for channel number and temperature assuming Q_{10} = 3.0.

activation (time constants of roughly 500 and 3,000 ms at −15 mV), neither these investigators nor Bennett et al. (1985) observed the earlier component associated with sigmoidal activation seen in our data and in other work from non-Purkinje preparations: e.g., guinea pig ventricular myocytes (Snyders et al., 1986; Matsuura et al., 1987) or frog atrium (Brown et al., 1976; Hume and Uehara, 1985; Simmons et al., 1986). However, in Purkinje tissues, the experimental conditions (possible

contaminating transient outward current, pacemaker currents, or calcium currents) may have prevented detection of an early sigmoidal component ($\tau \leq 100$ ms) associated with I_K activation. Hence, our results indicating that the C-C-O model accommodates the two later components of I_K activation but not the early activation delay (Fig. 6 *a*) are consistent with earlier studies where this model has been employed. Addition of a third closed state allows reproduction of all kinetic features of I_K activation, including early sigmoidal activation and the two later components (Fig. 6 *b*).

To account for the sigmoidal nature of I_K activation, several investigators have used n^2 Hodgkin-Huxley models: Hume et al. (1986) and Simmons et al. (1986) in frog atrium; and Matsuura et al. (1987) in guinea pig ventricular cells. Although the differences between our data and those from frog atrium may result from species differences, the study by Matsuura and co-workers (1987) was performed with the same preparation used here. Notably, the period of activation analyzed in their study included only the first 1,000 ms of I_K activation, a period considerably shorter than

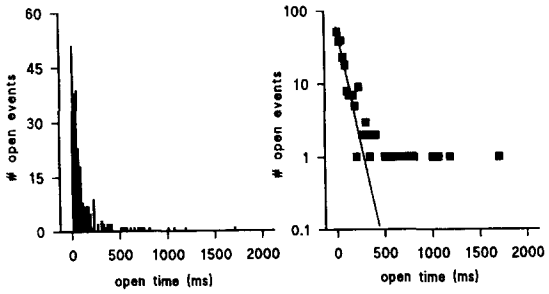

FIGURE 12. (*Left*) Histogram showing the distribution of open times (histogram contains events from both patches; bin size = 20 ms). (*Right*) The open times (■) were fitted to two exponentials ($\tau_1 = 70$ ms, $\tau_2 = 642$ ms). The first exponential is shown by the fitted line (log axis); the second exponential was underestimated due to the low number of events and the length of the clamp step (2 or 3.5 s; see Fig. 10).

that required for full activation (Fig. 5 *b* in Matsuura et al., 1988), even at the slightly higher temperatures used in their study (34–36°C). We have also shown that the n^2 model was adequate for a data set which is similarly reduced in duration (Fig. 5); however, such a model was inadequate if data from longer periods approaching steady-state activation were included. Our results indicated that I_K activation occurred with time constants ranging over approximately two orders of magnitude; to achieve this range of time constants with Hodgkin-Huxley gating kinetics, an $n^{\sim 100}$ model would be required due to the fixed relationship among the time constants in such models. Although we cannot exclude a parallel conductance model (Noble and Tsien, 1969; McDonald and Trautwein, 1978), in order to account for sigmoidal activation kinetics at least one of the two parallel conductances must have multiple closed states preceding the open state. Further, previous work in Purkinje tissue (Bennett et al., 1985) suggests that both conductances have the same reversal potential. Therefore, it seems unnecessary to postulate the existence of multiple channel types to explain the observed behavior.

Rate Constant Estimation through Global Fitting: Predictions of Single Channel Behavior

We globally fitted the four-state Markovian chain model to six sets of macroscopic data from six different voltage-clamped guinea pig ventricular myocytes. A representative fit is shown in Fig. 7; notably, the model is capable of representing the general features of I_K over a broad voltage range. The fits were qualitatively least satisfying at the voltage extremes (−80 and +70), and as predicted from previous evaluation of the global fitting procedure with simulated data (Balser et al., 1990), the errors in extracting rate constants were greatest at boundary voltages (Fig. 8). We have speculated that this phenomenon at boundary voltages results from the decrease in overlapping kinetic information from data at nearby voltages. However, as discussed in the Methods, voltage clamp errors may be larger at voltages where I_K is large (+70 mV), and may also contribute to the fit errors at these limits. The errors in the rate constants were greatest at positive voltages for those rate constants controlling movement from open to closed states, whereas the errors were greatest at negative voltages for rate constants controlling movement from closed to open states. Thus, as shown in previous work evaluating the global fitting procedure (Balser et al., 1990), and as one might predict, the rate constants were best defined at membrane potentials where they greatly influenced P_{open}.

An interesting observation was that pairs of forward and reverse rate constants may be voltage dependent in the same direction (k_{12} and k_{21}, k_{34} and k_{43}). Closer inspection of Fig. 8, however, reveals that the relative magnitudes of these rate constants also change with voltage; hence, at positive voltages k_{43} (opening direction) was larger than k_{34} (closing direction), and at negative potentials k_{12} (closing direction) was larger than k_{21} (opening direction). Thus, the relative magnitudes of all six voltage-dependent rate constants determine the behavior of the system; this demonstrates the difficulty with making "intuitive" assumptions regarding the voltage dependence of the rate constants in a complex system (Balser et al., 1990). The rate constants exhibiting the greatest voltage dependence (k_{12} and k_{32}) were those leaving the middle closed state (state C_2 in model 5, Table I). Hence the free energy change required to leave this state was heavily influenced by membrane potential. This may suggest that the residence time in this state depends on movement of charges in the transmembrane protein.

Global fits using a three-term parameterization for the rate constants (Eq. 5*a*) were significantly better than those where the squared voltage dependence was excluded (Eq. 5*b*). A squared voltage dependence was also noted by Bennett et al. (1985) in their assessment of I_K kinetics in Purkinje strands, and suggests that induced dipole forces are important modulators of delayed rectifier gating. The voltage dependence of the log transform of the rate constant controlling movement into the open state (k_{43}) was highly nonlinear. This further supports the concept that channel opening was influenced by membrane field-induced dipoles within the channel protein.

A gating model is useful when it can be used to make testable predictions about channel behavior. The predicted channel open time at +70 mV was 6.5 s. Hence, kinetic analysis of whole-cell delayed rectifier currents predicted single-channel openings of long duration; similar openings were detected in the single channel

records (Figs. 10 and 12). The predicted relationship between steady-state ($t = 200$ s) P_{open} and membrane potential (Fig. 9) was similar to that determined from fitting macroscopic current tails to a Boltzmann distribution (Fig. 2); the activation threshold was -20 mV, and activation saturated at $+70$ mV. The half-maximal voltage ($+26$ mV) was positive to that determined by other investigators (Matsuura et al., 1987; -13 mV) from tail amplitudes measured in guinea pig ventricular myocytes. However, they did not block the La^{3+}-sensitive current component, and we have repeatedly observed that outward tails do not satisfy the envelope test under these conditions. Occasionally, small deactivating outward tails were observed in solutions that did not contain La^{3+} after clamp steps to voltages where no time-dependent outward current developed (voltages below the I_K activation threshold). Such tails may represent deactivation of a transient outward current. In our experiments directed at assessing the whole-cell kinetics of the delayed rectifier, the concentration of La^{3+} in the external solutions was 30 μM. In bullfrog atrial cells, 10 μM La^{3+} had no effect on the kinetics, amplitude, or voltage dependence of I_K (Nathan et al., 1988); however, significant effects were noted at 500 μM concentrations. Further, in solutions that contain no La^{3+}, we obtain activation curves that are more positive than those reported by Matsuura et al.; hence, the difference between our results and those of Matsuura et al. does not entirely result from a La^{3+}-induced shift in the voltage dependence of delayed rectifier activation.

Single-Channel Delayed Rectifier Recordings

The most recent advances in our understanding of the molecular basis of cellular excitability have resulted from single channel recording (Hamill et al., 1981). Although this technique has been successfully applied to the study of cardiac inward rectifier K channels (Sakmann and Trube, 1984), measurements of delayed rectifier K channels in mammalian ventricle have remained elusive. Since catecholamines enhance the whole-cell delayed rectifier current (Bennett and Begenisich, 1987), in both cell-attached patches (Fig. 10) we used isoproterenol (2 μM) in the external solutions. In the presence of isoproterenol, delayed rectifier whole-cell currents at $+60$ mV are typically ≥ 1 nA. Assuming the cell dimensions described previously (radius = 10μM, length = 120 μM), and a single-channel current of 0.75 pA at $+60$ mV, the density of channels on the cell membrane should be approximately 18 channels/100 μm^2. While this density is somewhat lower than that of inward rectifier potassium channels (55 channels/100 μm^2; Sakmann and Trube, 1984), it does not explain the extreme rarity of observing these channels in cell-attached patches, nor does it account for the disappearance of channel activity after brief observation periods. Similar unexplained instability has been noted for cell-attached patch recordings of native *Shaker* A-type potassium channels from cultured *Drosophila* embryonic myotubes (Zagotta et al., 1989).

Similarly, a discrepancy exists between the ensemble probability of channel opening at $+60$ mV in the cell-attached patches ($P_{open} \geq 0.2$, Fig. 10) and the analysis of whole-cell delayed rectifier steady-state current-voltage relationships ($P_{open} > 0.9$, Figs. 2 and 9). The reason for the lower probability of channel opening for cell attached patches is unclear. It is possible that the same phenomena which are responsible for the extremely low probability of detecting single delayed rectifier

channels and recording them for long periods also underlies the low probability of channel opening in patches where they are rarely and fortuitously observed. Recent studies have demonstrated that patch electrode glass composition may effect the ion channel current–voltage relationship (Cota and Armstrong, 1988; Furman and Tanaka, 1988); such effects were minimized in those studies by using ≥ 10 mM EGTA in the electrode, which presumably chelated multivalent cations released by the glass. Although 11 mM EGTA was present in the electrodes for our whole-cell experiments, no EGTA was used for cell-attached patches since we did not wish to expose the external face of the ion channel to abnormally low levels of divalent cation. Our electrodes were made from a borosilicate glass, which minimized these artifacts in whole-cell K current recordings from rat pituitary cells (Cota and Armstrong, 1988); however, we cannot exclude the possibility that this harder variety of glass releases substances that interfere with K channel opening in our patches. An alternative explanation is that glass–membrane interfacial forces stress the membrane patch and alter channel function (Furman and Tanaka, 1988). Such effects on ion channels near the patch electrode would not be detectable in whole-cell current measurements for cells as large as these.

When the patch was depolarized to +60 mV, the channels opened after a delay. Analysis of the time to first opening (latency) gave distributions which had a maximum value at a time later than zero (Fig. 11), providing single-channel evidence for the existence of multiple closed states preceding the open state (Patlak and Horn, 1982). Although the predicted latency distributions from analysis of the whole-cell currents using the C-C-C-O model agreed well with the single-channel distributions, it was not feasible to use the measured latency distributions to discriminate among models with various numbers of closed states owing to the low number of recorded events. Further, since both patches contained multiple channels, unambiguous quantitative analysis of closed times was not feasible. However, inspection of the records from Fig. 10 suggests the presence of at least three components; these included very brief closures within long openings (≤10 ms), short intervals between openings (50–500 ms), and very long closures (≥2 s; sweeps that contained no openings). These components are consistent with a kinetic model having three closed states, as suggested by analysis of the whole-cell delayed rectifier currents.

Analysis of amplitude histograms (Fig. 11) for the two patches gave a mean chord conductance of 5.4 pS (V_m measured at V_{rest} + 140 mV: $V_m \sim +60$ mV). There are currently no other reports of single-channel delayed rectifier currents from mammalian ventricle with which to compare these values. In mammalian cardiac cells the only single-channel studies of a delayed rectifier K channel have been in the nodal pacemaker cells of rabbit heart (Shibasaki, 1987). In contrast to the outward currents we have recorded, Shibasaki studied inward K currents using elevated pipette K concentrations. Under these conditions a single channel conductance of 11.1 pS was observed at $[K]_o$ = 150 mM, and this value varied in proportion to the square root of $[K]_o$ from 100 to 300 mM. Extrapolation of this relationship to the more physiologic $[K]_o$ we utilized (4.5 mM) gives 1.9 pS, considerably lower than the chord conductance we observed. There are no data to indicate how G_K for the delayed rectifier in ventricle depends on $[K]_o$, especially at low concentrations. Further, the nodal channel inactivates (Shibasaki, 1987), whereas there is no

evidence in this or previous studies (Matsuura et al., 1987) to suggest that I_K in ventricle inactivates. These differences suggest that the nodal K channels differ qualitatively from those in ventricle. Embryonic chick ventricle has a larger conductance channel (15 pS in $[K]_o$ = 4.0 mM) which may underlie I_K in that species (Clapham and Logothetis, 1988). Notably, the delayed rectifier channel from avian hepatocytes has recently been shown to have a slope conductance of 6 pS in cell-attached patches (Marchetti et al., 1988). This channel, however, was fully activated in 200 ms, whereas delayed rectifier channels in cardiac cells require several seconds to fully activate.

Visual inspection of the records as well as analysis of the open times (Fig. 12) suggests multiple types of opening behavior for these channels. Although the longer component is underestimated due to the low number of events and the short duration of the clamp step, there is clearly a tendency for long openings on the order of seconds as predicted by the kinetic analysis of the whole-cell currents. The shorter openings may be explained by block of the channel by one or more ions in the solution, or by a kinetic feature that is obvious at the single-channel level, but which could not be deduced from analysis of the macroscopic currents. In addition, openings of intermediate amplitude were noted at approximately one-half the main unitary current level (Fig. 12); examination of the single-channel records reveals long openings to sublevels (Fig. 10). Subconductance openings have recently been reported for cloned delayed rectifier K channels from rat brain expressed in both *Xenopus* oocytes (Stühmer et al., 1988) and in a mammalian muscle cell line (Liman et al., 1989). The subconductance openings in our study appeared relatively infrequently; hence, these openings do not explain the short open times which are prominent in the open time histogram. These results suggest that in addition to three closed states, a full model for delayed rectifier gating should include multiple open states.

Implications for Potassium Channel Structure

Recent advances in the elucidation of K channel structure have been derived from expression of the *Shaker* gene of *Drosophila* in *Xenopus* oocytes (Timpe et al., 1988; Schwarz et al., 1988), which codes for an inactivating A-type K channel; the 70-kD protein subunits are thought to assemble in groups to form potassium channels. Although it is possible to reconstitute K channel behavior using only one class of *Shaker* subunits, several classes of proteins may be produced through alternative splicing. Multiple types of subunits may therefore be present in the native cell, and it has been suggested that native K channels might consist of heterologous subunits (Timpe et al., 1988; Schwarz et al., 1988). Our data indicate that gating of the delayed rectifier in cardiac cells cannot be explained by Hodgkin-Huxley models, which require that gating particles or subunits are functionally identical and independent. Hence, the gating subunits for the cardiac channel may be either different (heterologous subunits), or functionally coupled, as suggested by Begenisich (1979) in his study of the delayed rectifier in frog node of Ranvier. Future studies that combine the expanding capabilities of molecular biology with electrophysiologic studies (Stühmer et al., 1989) should provide important clues to the structure–function relationships in delayed rectifier K channel gating.

The authors wish to thank Drs. Luc Hondeghem and Dirk Snyders for suggestions and discussion, and Dr. James Davis and Mrs. Holly Gray for technical assistance.

This work was supported by grants from The American Heart Association (Tennessee Affiliate), the National Institutes of Health (HL-32694 and HL-40608), and the Stahlman Cardiovascular Research Endowment. J. R. Balser was supported by an institutional award from the Medical Scientist Training Program (GM07374).

Original version received 26 February 1990 and accepted version received 23 April 1990.

REFERENCES

Armstrong, C. M. 1975. Interaction of tetraethylammonium ion derivatives with the potassium channels of giant axons. *Journal of General Physiology.* 58:413–437.

Balser, J. R., D. M. Roden, and P. B. Bennett. 1990. Global parameter optimization for cardiac potassium channel gating models. *Biophysical Journal.* 57:433–444.

Begenisich, T. 1979. Conditioning hyperpolarization-induced delays in the potassium channels of myelinated nerve. *Biophysical Journal.* 27:257–266.

Bennett, P. B., and T. B. Begenisich. 1987. Catecholamines modulate the delayed rectifying potassium current (I_K) in guinea pig ventricular myocytes. *Pflügers Archiv.* 410:217–219.

Bennett, P. B., L. C. McKinney, R. C. Kass, and T. B. Begenisich. 1985. Delayed rectification in the calf cardiac Purkinje fiber. Evidence for multiple state kinetics. *Biophysical Journal.* 48:553–567.

Brown, H. F., A. Clark, and S. J. Noble. 1976. Identification of the pacemaker current in frog atrium. *Journal of Physiology.* 258:521–545.

Clapham, D. E., and L. J. DeFelice. 1985. Voltage-activated K channels in embryonic chick heart. *Biophysical Journal.* 45:40–42.

Clapham, D. E., and D. E. Logothetis. 1988. Delayed rectifier K^+ current in embryonic chick heart ventricle. *American Journal of Physiology.* 254:H192–H197.

Clark, R. B., W. R. Giles, and Y. Imaizumi. 1988. Properties of the transient outward current in rabbit atrial cells. *Journal of Physiology.* 405:147–168.

Cohen, I. S., N. B. Datyner, G. A. Gintant, and R. P. Kline. 1986. Time-dependent outward currents in heart. *In* the Heart and Cardiovascular System. H. A. Fozzard et al., editors. Raven Press, New York.

Cole, K. S., and J. W. Moore. 1960. Potassium ion current in the squid giant axon: dynamic characteristic. *Biophysical Journal.* 1:1–14.

Colquhoun, D., and F. J. Sigworth. 1983. Fitting and statistical analysis of single-channel records. *In* Single-Channel Recording. B. Sakmann and E. Neher, editors. Plenum Press, New York. 191–263.

Conti, F., and E. Neher. 1980. Single channel recordings of K^+ currents in squid axons. *Nature.* 285:140–143.

Coraboeuf, E., and E. Carmeliet. 1982. Existence of two transient outward currents in sheep cardiac Purkinje fibers. *Pflügers Archiv.* 392:352–359.

Cota, G., and C. M. Armstrong. 1988. Potassium channel "inactivation" induced by soft-glass patch pipettes. *Biophysical Journal.* 53:107–109.

Duchatelle-Gourdon, I., H. C. Hartzell, and A. A. Lagrutta. 1990. Modulation of the delayed rectifier potassium current in frog cardiomyocytes by β-adrenergic agonists and magnesium. *Journal of Physiology.* In press.

Farmer, B. B., M. Mancina, E. Williams, and A. Watanabe. 1983. Isolation of calcium tolerant

myocytes from adult rat heart: review of the literature and description of a method. *Life Sciences.* 33:1–18.

Furman, R. E., and J. C. Tanaka. 1988. Patch electrode glass composition affects ion channel currents. *Biophysical Journal.* 53:287–292.

Furukawa, T., Y. Tsujimura, K. Kitamura, H. Tanaka, and Y. Habuchi. 1989. Time- and voltage-dependent block of the delayed K^+ current by quinidine in rabbit sinoatrial and atrioventricular nodes. *The Journal of Pharmacology and Experimental Therapeutics.* 251:756–763.

Gintant, G. A., N. B. Datyner, and I. S. Cohen. 1985. Gating of delayed rectification in acutely isolated canine cardiac Purkinje myocytes; evidence for a single voltage-gated conductance. *Biophysical Journal.* 48:1059–1064.

Godfrey, K. 1985. Statistics in practice: comparing the means of several groups. *New England Journal of Medicine.* 313:1450–1456.

Hamill, O. P., A. Marty, E. Neher, B. Sakmann, and F. J. Sigworth. 1981. Improved patch clamp techniques for high-resolution current recording from cells and cell-free membrane patches. *Pflügers Archiv.* 391:85–100.

Hille, B. 1977. Local anesthetics: hydrophilic and hydrophobic pathways for the drug-receptor reaction. *Journal of General Physiology.* 69:497–515.

Hindmarsh, A. C. 1983. Odepack, a systematized collection of ode solvers. *In* Scientific Computing. R. S. Stepleman, editor. North-Holland Publishing Co., Amsterdam. 55–64.

Hodgkin, A. L., and A. F. Huxley. 1952. A quantitative description of membrane current and its application to conduction and excitation in nerve. *Journal of Physiology.* 117:500–544.

Hondeghem, L. M., and B. H. Katzung. 1977. Time and voltage-dependent interactions of antiarrhythmic drugs with cardiac sodium channels. *Biochimica et Biophysica Acta.* 472:373–398.

Horn, R. 1987. Statistical methods for model discrimination; applications to gating kinetics and permeation of the acetylcholine receptor channel. *Biophysical Journal.* 51:255–263.

Hume, J. R. 1989. Properties of myocardial K^+ channels and their pharmacological modulation. *In* Molecular and Cellular Mechanisms of Antiarrhythmic Agents. L. Hondeghem, editor. Futura Publishing Co., Inc., Mount Kisco, NY. 113–131.

Hume, J. R., and W. Giles. 1983. Ionic currents in single isolated bullfrog atrial cells. *Journal of General Physiology.* 83:153–194.

Hume, J. R., W. Giles, K. Robinson, E. F. Shibata, R. D. Nathan, K. Kanai, and R. Rasmusson. 1986. A time- and voltage-dependent K current in single cardiac cells from bullfrog atrium. *Journal of General Physiology.* 88:777–798.

Hume, J. R., and A. Uehara. 1985. Ionic basis of the different action potential configurations of single guinea-pig atrial and ventricular myocytes. *Journal of Physiology.* 368:525–544.

Josephson, I. R., J. Sanchez-Chapula, and A. M. Brown. 1984. Early outward current in rat single ventricular cells. *Circulation Research.* 54:157–162.

Kim, D., A. Okada, and T. W. Smith. 1987. Control of cytosolic calcium activity during low sodium exposure in cultured chick heart cells. *Circulation Research.* 61:29–41.

Lecar, H., and T. G. Smith. 1985. Voltage clamping small cells. *In* Voltage and Patch Clamping with Microelectrodes. T. G. Smith, H. Lecar, S. J. Redman, and P. W. Gage, editors. Waverly Press, Inc., Baltimore, MD. 231–256.

Liman, E. R., G. Koren, B. Nadal-Ginard, and P. Hess. 1989. Stable expression in a mammalian muscle cell line of a cloned delayed rectifier K^+ channel from rat brain. *Circulation.* 80:1585.

Marchetti, C., R. T. Premont, and A. M. Brown. 1988. A whole-cell and single-channel study of the voltage-dependent outward potassium current in avian hepatocytes. *Journal of General Physiology.* 91:255–274.

Mathias, R. T., B. R. Eisenberg, N. B. Datyner, G. A. Gintant, and I. S. Cohen. 1985. Impedance and morphology of isolated canine cardiac Purkinje myocytes: comparison with intact strand preparations. *Biophysical Journal.* 47(2, Pt. 2):499a. (Abstr.)

Matsuura, H., T. Ehara, and Y. Imoto. 1987. An analysis of the delayed outward current in single ventricular cells of the guinea-pig. *Pflügers Archiv.* 410:596–603.

Matsuda, H., and A. Noma. 1984. Isolation of calcium current and its sensitivity to monovalent cations in dialysed ventricular cells of guinea-pig. *Journal of Physiology.* 57:553–573.

McDonald, T. F., and W. Trautwein. 1978. The potassium current underlying delayed rectification in cat ventricular muscle. *Journal of Physiology.* 274:217–246.

Nathan, R. D., K. Kanai, R. B. Clark, and W. Giles. 1988. Selective block of calcium current by lanthanum in single bullfrog atrial cells. *Journal of General Physiology.* 91:549–572.

Nelder, J. A., and R. Mead. 1965. A simplex method for function minimization. *Computer Journal.* 7:308–313.

Noble, D., and R. W. Tsien. 1969. Outward membrane currents activated in the plateau range of potentials in cardiac Purkinje fibres. *Journal of Physiology.* 200:205–231.

Palti, Y., G. Ganot, and R. Stampfli. 1976. Effect of conditioning potential on potassium current kinetics in the frog node. *Biophysical Journal.* 16:261–273.

Patlak, J., and R. Horn. 1982. Effect of N-bromoacetamide on single sodium channel currents in excised membrane patches. *Journal of General Physiology.* 79:333–351.

Petzold, L. R. 1983. Automatic selection of methods for solving stiff and nonstiff systems of ordinary differential equations. *Society for Industrial and Applied Mathematics Journal on Scientific and Statistical Computing.* 4:136–148.

Roden, D. M., P. B. Bennett, D. J. Snyders, J. R. Balser, and L. M. Hondeghem. 1988. Quinidine delays I_K activation in guinea pig ventricular myocytes. *Circulation Research.* 62:1055–1058.

Saigusa, A., and H. Matsuda. 1988. Outward currents through the inwardly rectifying potassium channel of guinea-pig ventricular cells. *Japanese Journal of Physiology.* 38:77–91.

Sakmann, B., and G. Trube. 1984. Conductance properties of single inwardly rectifying potassium channels in ventricular cells from guinea-pig heart. *Journal of Physiology.* 347:641–657.

Sanguinetti, M. C., and N. K. Jurkiewicz. 1990. Two components of cardiac delayed rectifier K^+ current. *Journal of General Physiology.* 96:195–215.

Schwarz, T. L., B. L. Tempel, D. M. Papazian, Y. N. Jan, L. Y. Jan. 1988. Multiple potassium-channel components are produced by alternative splicing at the *Shaker* locus in *Drosophila. Nature.* 331:137–142.

Shibasaki, T. 1987. Conductance and kinetics of delayed rectifier potassium channels in nodal cells of the rabbit heart. *Journal of Physiology.* 387:227–250.

Shoup, T. E. 1983. Numerical Methods for the Personal Computer. Prentice-Hall, Inc., Englewood Cliffs, NJ. 174–185.

Simmons, M. A., T. Creazzo, and H. C. Hartzell. 1986. A time-dependent and voltage-sensitive K^+ current in single cells from frog atrium. *Journal of General Physiology.* 88:739–755.

Snyders, D. J., L. M. Hondeghem, and B. G. Katzung. 1986. Sigmoidal time course of I_K activation in cardiac myocytes. *Circulation.* 74:SII–255.

Stevens, C. F. 1978. Interactions between intrinsic membrane protein and electric field; an approach to studying nerve excitability. *Biophysical Journal.* 22:295–306.

Stühmer, W., M. Stocker, B. Sakmann, P. Seeburg, A. Baumann, A. Grupe, and O. Pongs. 1988. Potassium channels expressed from rat brain cDNA have delayed rectifier properties. *Federation of European Biochemical Societies Letters.* 242:199–206.

Stühmer, W., F. Conti, H. Suzuki, X. Wang, M. Noda, N. Yahagi, H. Kubo, and S. Numa. 1989. Structural parts involved in activation and inactivation of the sodium channel. *Nature.* 339:597–603.

Timpe, L. C., T. L. Schwarz, B. L. Tempel, D. M. Papazian, Y. N. Jan, and L. Y. Jan. 1988. Expression of functional potassium channels from *Shaker* cDNA in *Xenopus* oocytes. *Nature.* 331:143–145.

Wendt-Gallitelli, M. F., and G. Isenberg. 1985. Extra- and intracellular lanthanum: modified calcium distribution, inward currents and contractility in guinea pig ventricular preparations. *Pflügers Archiv.* 405:310–322.

Young, S. H., and J. W. Moore. 1981. Potassium ion currents in the crayfish giant axon; dynamic characteristics. *Biophysical Journal.* 36:723–733.

Zagotta, W. N., T. Hoshi, and R. W. Aldrich. 1989. Gating of single *Shaker* potassium channels in *Drosophila* muscle and in *Xenopus* oocytes injected with *Shaker* mRNA. *Proceedings of the National Academy of Sciences USA.* 86:7243–7247.